A copper(II) chloride coordination compound with an adamantane-like core

Benjamin A. Mukda,[a] Christopher P. Landee,[b] Melanie Rademeyer,[c] Mark M. Turnbull[a*] and Brian M. Wells[d]

[a] Carlson School of Chemistry and Biochemistry and [b] Department of Physics, Clark University, 950 Main St., Worcester, MA 01610, USA; MTurnbull@clarku.edu

[c] Department of Chemistry, University of Pretoria, Private Bag X20, Hatfield 0028, South Africa

[d] Department of Physics, University of Hartford, 200 Bloomfield Ave, West Hartford, CT 06117 USA

Abstract

A new tetracopper(II) coordination compound, $[Cu_4Cl_6O(iQuin)_4]$ (**1**, iQuin = isoquinoline) with an adamantane-like structure is reported. The compound crystallizes in the tetragonal space group P4/n with one crystallographically unique Cu(II) and oxide ions, and two chloride ions. Variable temperature magnetic measurements reveal dominant antiferromagnetic interactions, but the crystal structure suggests the likelihood of magnetic frustration in the compound. Modeling results indicate the presence of two competing interactions, $J_{ap}/k_B = -61.1(7)$ K and $J_{eq}/k_B = 41.2(3)$ K, (ap = apical; eq = equatorial) as well as a Zeeman coupling of the Cu(II) ions with the external magnetic field. All data were fit using the Hamiltonian $\hat{H} = J_1 \sum_{i=1}^{6} \hat{S}_{\gamma_i(1)} \cdot \hat{S}_{\gamma_2(2)} + J_2 \sum_{i=1}^{6} \left(\hat{S}_{\alpha_i(1)} \cdot \hat{S}_{\alpha_i(2)} + \hat{S}_{\beta_i(1)} + \hat{S}_{\beta_i(2)}\right) + g\mu_B \vec{H} \cdot \sum_{j=1}^{4} \hat{S}_j$.

Introduction

Since the first report of transition-metal based inorganic cage structures that resemble adamantane (henceforth, adamantoids) [1], these compounds have been isolated and prepared via a variety of synthetic routes. The basic structure has a transition metal ion occupying the tertiary sites (see Figure 1), halide ions occupying the secondary sites and most often an oxide ion at the center, giving the general formula $[M_4X_6O(L)_4]$ (where L is an ancillary ligand,

external to the cage structure) [2]. 'Hollow' structures, those lacking the central oxide ion, have also been reported [3]. The ligand L fills out the coordination sphere of the metal ion and can be a variety of species including N [4], O [5], X [6] and even bridging ligands [3d]. Both P_4O_6 and P_4O_{10} have similar structures, lacking the central oxide, with phosphorus atoms in place of the transition metal ions and oxide ions in place of the halide ions/ancillary ligands [7].

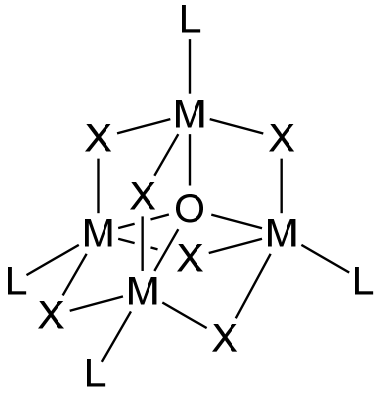

Figure 1. Basic structure of the adamantoid core.

Magnetic interactions within the adamantoid core are propagated via superexchange through both the bridging halide ions and central oxide ion. However, detailed analysis of the magnetic properties of these materials has been limited [8]. A large majority of these compounds crystallize in low-symmetry space groups (such as P-1) rendering the potential superexchange pathways too numerous for detailed analysis. A small number have been reported in higher symmetry space groups such as F-43c [9] and I-43m [10].

In the course of our investigations of copper(II) halide complexes of a variety of N-donor ligands [11] we encountered the serendipitous preparation of such an adamantoid with isoquinoline as the ancillary substituent. The compound crystallized in the tetragonal space group *P4/n* making it suitable for the study of its magnetic properties. We report here the synthesis, structure, magnetic properties and theoretical magnetic analysis of $[Cu_4Cl_6O(iQuin)_4]$ (**1**, iQuin = isoquinoline).

Experimental

Copper (I) oxide was acquired from J.T. Baker. Copper (II) chloride dihydrate was acquired from Mallinckrodt Chemicals. Isoquinoline was acquired from Acros Organics. 1-

Butanol was acquired from Fisher Scientific. All materials were used as received. Infrared spectra were recorded via ATM on a Perkin-Elmer Spectrum 100 infrared spectrophotometer. Powder X-ray diffraction data were collected using a Bruker D8 Advance powder diffractometer. Elemental analysis was performed at the Marine Science Institute, University of California Santa Barbara, CA.

Synthesis of tetra(isoquinoline)hexa-μ-chlorido-μ4-oxotetracopper(II), **1**

$CuCl_2 \cdot 2\ H_2O$ (0.542 g, 3.18 mmol), CuO (0.073g, 0.92 mmol), and iQuin (0.513g, 3.97 mmol) were added to a round-bottom flask. 50 mL of 1-butanol was then added to the flask and refluxed for one week, after which brown precipitate was visible in the flask. This precipitate was collected via vacuum filtration, washed with room temperature 1-butanol, and allowed to dry to yield 0.241 g (26.2%). CHN for $C_{36}H_{28}N_4OCl_6Cu_4$ obs(calcd): C, 42.97(43.26); H, 2.77(2.83); N, 5.78(5.60). IR: 1633 m, 1598 w, 1500 w, 1386 m, 1278 m, 1148 w, 1066 m, 964 w, 823 s, 751 m, 635 m, 582 m cm^{-1}.

Crystals suitable for single-crystal X-ray diffraction were grown from a solution of $Cu(iQuin)_2Cl_2$ [11a] in DMF by vapor diffusion of 1-propanol into the solution over the course of six weeks.

Magnetic data collection:

Data for **1** were collected on a Quantum Design MPMS SQUID magnetometer. Crystals were powdered, packed into a gelatin capsule and mounted in a plastic straw. The magnetization of the sample was measured as a function of field from 0 – 50 kOe at 1.8 K. Five data points were recollected as the field returned to 0 Oe. No hysteresis effects were observed. The magnetization of the sample was then measured in a 1 kOe applied field from 1.8 – 310 K. Data were corrected for the diamagnetic contributions of the constituent atoms as estimated from Pascal's constants [12], the contributions from the sample holder (measured independently) and the temperature independent paramagnetism of the Cu(II) ion. The Hamiltonian

$$\widehat{H} = J_1 \sum_{i=1}^{6} \hat{S}_{\gamma_i(1)} \cdot \hat{S}_{\gamma_2(2)} + J_2 \sum_{i=1}^{6} \left(\hat{S}_{\alpha_i(1)} \cdot \hat{S}_{\alpha_i(2)} + \hat{S}_{\beta_i(1)} + \hat{S}_{\beta_i(2)} \right) + g\mu_B \vec{H} \cdot \sum_{j=1}^{4} \hat{S}_j$$

was employed for all fitting. Powder X-ray diffraction data were compared to the calculated pattern based on the single crystal structure (Figure SI-1) to verify the phase of the sample and purity. No impurities were observed.

X-ray Structure Determination:

Data collection was carried out on a Bruker D8 Venture diffractometer fitted with a Photon 100 CMOS detector employing graphite-monochromated Mo-Kα radiation, using φ and ω scans. Using the SAINT+ software [13], the data were reduced and absorption corrections were made using the SADABS program [14]. Structure solution was carried out using the program SHELXS-2014 [15] while refinements were performed using SHELXL-2018 [16]. Non-hydrogen atoms were refined using anisotropic thermal parameters. Hydrogen atoms were placed in their geometrically calculated positions and refined as a riding model with fixed isotropic thermal parameters. Attempts to remove the trace electron density in the solvent accessible voids via SQUEEZE did not improve the refinement and as such were left as originally found. The final residual peak (1.09 e/Å^3) lies 1.91 Å from the central oxide ion. Crystallographic information for compound **1** may be found in Table 1. Selected bond lengths and angles are given in Table 2. The structure of **1** has been deposited with the CCDC as #2249833.

Table 1. Crystal data and structure refinement for **1** .

Empirical formula:	$C_{36}H_{28}N_4OCl_6Cu_4$
Formula weight (g/mol)	999.48
Crystal system	Tetragonal
Space group	*P4/n*
Unit cell dimensions:	
a (Å)	15.0659(9)
b (Å)	15.0659(9)
c (Å)	8.9209(9)
Volume (Å^3)	2024.9(3)
Z	2
Density (calc) (Mg/m^3)	1.639
Size (mm)	0.16 x 0.16 x 0.05
F(000)	996
μ (mm^{-1})	2.502
Data collection:	
Temperature (K)	150(2)

Max., min. transmission	0.7786, 0.7141
Reflections collected	91498
Independent reflections	2539
θ range (°)	2.653 to 28.423
Range h, k, l	$-20 \le h \le 20$
	$-20 \le k \le 20$
	$-11 \le l \le 11$
Refinement:	
Data/restraints/parameters	2539/0/120
Goodness-of-fit on F^2	1.101
Final R indices [$I>2\sigma(I)$]	
R_1	0.0341
wR_2	0.0730
R indices (all data)	
R_1	0.0513
wR_2	0.0796
Largest difference peak (e/Å^3)	1.094
Largest difference hole (e/Å^3)	-0.494

Table 2: Bond lengths (Å) and angles (°) for **1**

Bond Lengths		Bond Angles	
Cu1-O1	1.9035(3)	O1-Cu1-Cl1	83.19(10)
Cu1-Cl1	2.372(4)	O1-Cu1-Cl1^A	84.21(11)
Cu1-Cl1^A	2.334(4)	O1-Cu1-Cl2	85.93(2)
Cu1-Cl2	2.3905(7)	O1-Cu1-Cl2^B	84.229(19)
Cu1-Cl2^B	2.4509(7)	O1-Cu1-N12	179.18(7)
Cu-N12	1.976(2)	Cu1-O1-Cu1^A	109.363(18)
		Cl1-Cu1-Cl2	120.18(8)
		Cl1-Cu1-Cl2^B	120.55(34)
	Ave.	N12-Cu1-Cl#	95.71(7)

Symm. Op. A = 0.5-x, 1.5-y, -z; B = 1-y, 0.5+x, 2-z.

Theoretical methods

All theoretical calculations and fitting were performed using MATLAB [17]. The anisotropic Hamiltonian, including Zeeman coupling with an external magnetic field, was chosen to model this system for an ideal tetrahedral geometry. Using the complete basis set for a tetramer, the 16×16 symbolic Hamiltonian matrix could be constructed. By diagonalizing this matrix, the energy eigenvalues and degeneracies are determined. Once known, the partition function is calculated. A script was written to numerically differentiate the partition function with respect to the magnetic field to obtain the magnetization and susceptibility functions. The theoretical

function for χT was then fit to experimental data by implementing a loop over varying fitting parameters using the least-squares curve fitting technique. This was done to ensure a global minimum. Numerical fitting values were plugged back into our theoretical equations and compared with experimental measurements. The anisotropic Hamiltonian, including Zeeman coupling with an external magnetic field, was chosen to model this system for an ideal tetrahedral geometry [18].

Results

Synthesis:

The initial preparation of **1** occurred during attempts to grow crystals of $Cu(iQuin)_2Cl_2$ [11a]. After identification of the compound by single crystal X-ray diffraction, methods for a direct synthesis were investigated. **1** was alternatively synthesized first via reaction of copper (II) dichloride with isoquinoline, both dissolved in 1-butanol in a cold room at 7° C. Addition produced an immediate precipitate that was left in the cold room for five days and was then refluxed for 5 days. This produced a black-green crust above a light green solution. The black-green crust, after collection via vacuum filtration was observed to be the desired product. Due to the difficulty of product purification and low yields, another route was investigated. This route involved using copper (I) oxide as the source of the central oxide ion (in combination with the metal halide salt) rather than what is believed to be the source of the ion, water [1]. Although water is generally accepted to be the source of the oxide ion in the center of the cage [2], water need not be specifically added to the reaction. Water may be introduced through hydrated metal salts, or simply through atmospheric moisture given the small scale of the reactions. This procedure produced complex **1**, but longer reflux times were seen to introduce larger amounts of unknown impurities.

X-Ray Structure:

Compound **1** crystallized in the tetragonal space group *P4/n* with two molecules per unit cell. The asymmetric unit (Figure 2a) comprises one Cu(II) ion, 0.25 oxide ion, 1.5 chloride ions and one coordinated isoquinoline (iQuin) molecule. The oxide ion is located in the center of a cage structure on both a glide plane and four-fold roto-inversion axis. It is bonded to four symmetry equivalent Cu(II) ions in general positions. Cl1 is two-site disordered (Figure 2b)

about a two-fold axis parallel to the *c*-axis, with 50:50 occupancies as required by symmetry. Only one site of the disordered ion is shown in all other figures for clarity. The iQuin ring is nearly planar (mean deviation of the constituent atoms = 0.0057 Å). Bond lengths and angles within the iQuin ring are comparable to those observed earlier for $Cu(iQuin)_2Br_2$ [11a] and $[Cu(iQuin)I]_n$ [19].

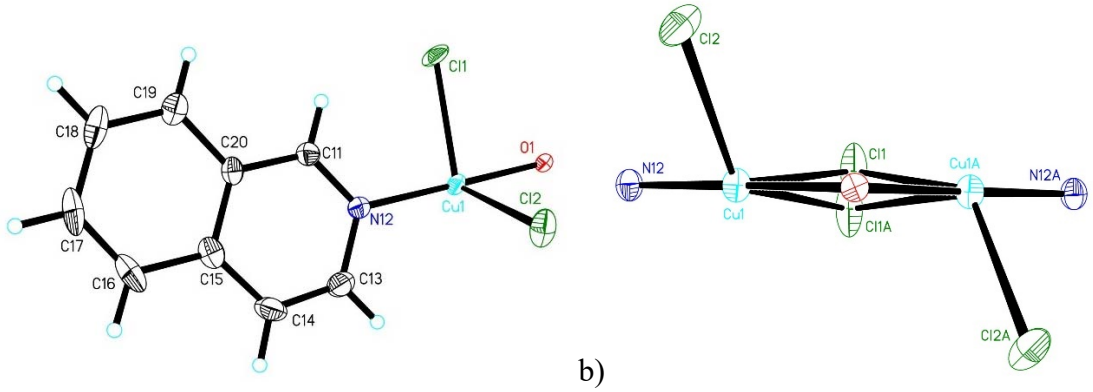

a) b)

Figure 2. a) Thermal ellipsoid plot of the asymmetric unit of **1** showing 50% probability ellipsoids. Hydrogen atoms are shown as spheres of arbitrary size. Only one position of the disordered Cl1 ion is shown. b) A view of the two-site disorder of Cl1, viewed parallel to the two-fold symmetry axis. (Symm. Op. A = 0.5-x, 1.5-y, z).

The overall structure of **1** is that of an adamantoid and is shown in Figure 3a. A fully labeled figure including only one iQuin molecule is shown in Figure SI-2. Cu1 exhibits a distored trigonal bipyramidal geometry with an Addison parameter of 0.79 [20] where the oxide ion and iQuin N atoms occupy the axial positions (Figure 3b). The O1-Cu1 bond length is 1.9035(3) Å while the O1-Cu1-Cl# angles are all slightly acute (range 83.2-85.9°) as has been observed in related copper chloride based adamantoids [21].

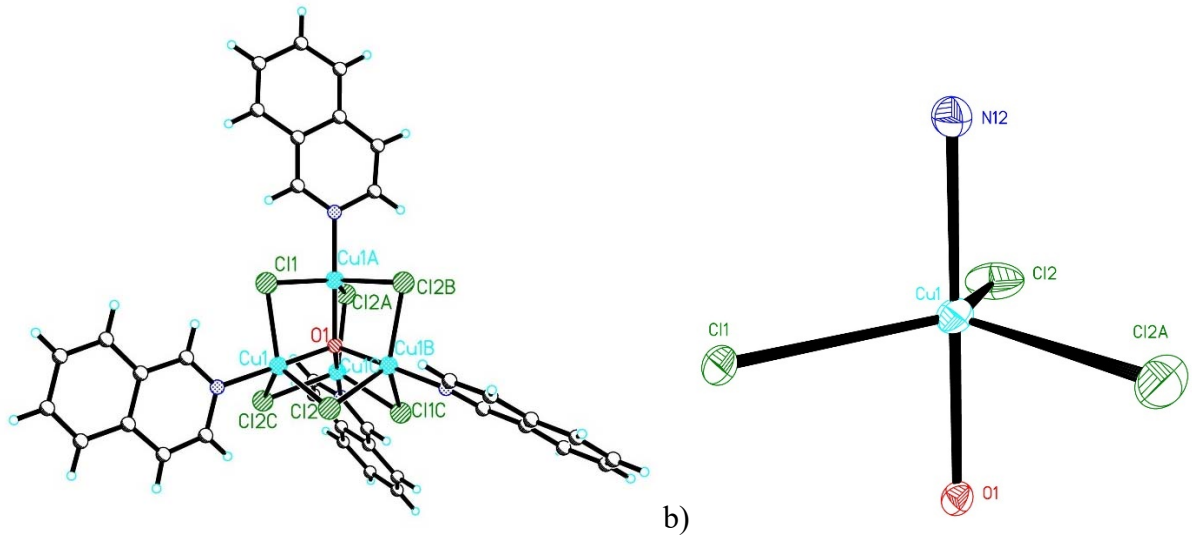

a) b)

Figure 3. a) The molecular structure of **1**. b) The coordination geometry of the Cu(II) ion. Symm. Ops. (both figures): A = 0.5-x, 1.5-y, z; B = y-0.5, 1-x, 2-z; C = 1-y, 0.5+x, 2-z.

Molecules of **1** packed in stacks parallel to the *c*-axis, with short Cl···Cl contacts [$d_{Cl...Cl}$ = 3.254 Å] linking the molecules into chains (Figure 4a). The structure is further stabilized by π-stacking interactions (Figure 4b) between the isoquinoline molecules in the *a*- and *b*-directions. The distance between ring centroids is 3.66 Å, the interplanar distance is 3.363 Å and the slip angle is 22.8°.

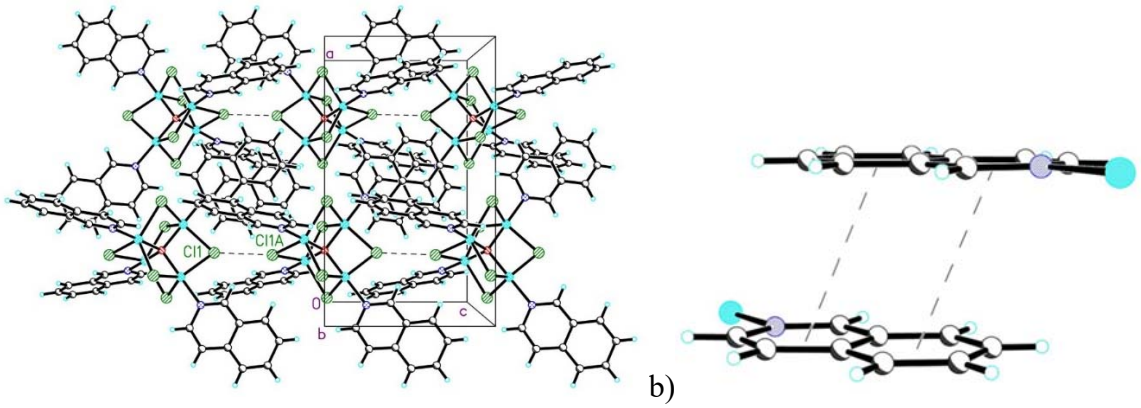

a) b)

Figure 4. a) Packing diagram of **1** viewed parallel to the *b*-axis. Dashed lines represent short Cl···Cl contacts. Symm. Op. A = 0.5-x, 1.5-y, -1-z. b) π-stacking of the iQuin rings. Dashed lines represent the vectors between the right centroids.

Solvent accessible voids of 118 $Å^3$ occur in the interstices between adamantoid units (see Figure SI-3). A small amount of residual electron density was located in the voids. Attempts to remove

the electron density via SQUEEZE did not improve the refinement.

Magnetic properties

Magnetization for **1** rises steadily with increasing field to a value of ~8,000 emu/mol (see Figure SI-4) at 50 kOe (the maximum field), well below the expected saturation value of ~23,000 emu/mol for four S = ½ Cu(II) ions, indicating the presence of antiferromagnetic interactions in the material. Somewhat surprisingly, due to the low value of M at 50 kOe, χ rises steadily with decreasing temperature from 310 K down to 1.8 K (see Figure SI-5) and no maximum is observed. The temperature dependency of χ is shown as (χT)T and 1/χ (T) in Figure 5.

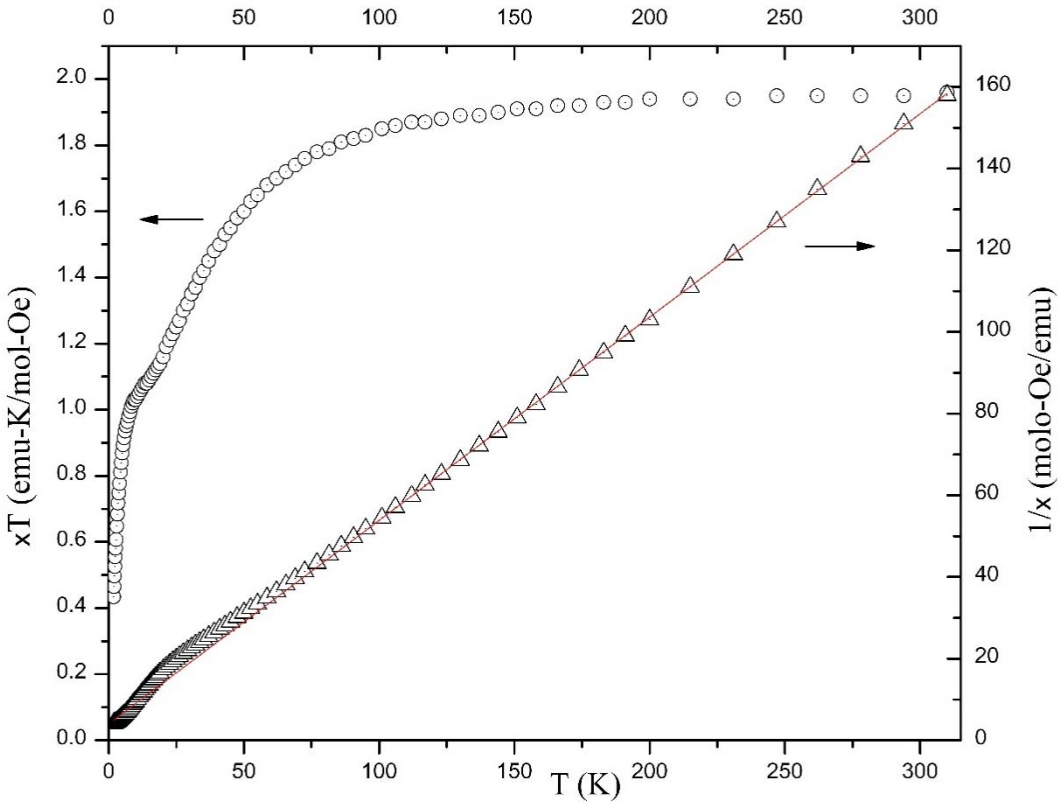

Figure 5. χT(T) (○) and 1/χ (T) (Δ) data for **1**. The solid line represents the fit to the Curie-Weiss law.

The 1/χ data above 80 K were fit to the Curie-Weiss law resulting in a Curie constant (CC) of 2.008(4) emu-K/mol-Oe, in good agreement with four S = ½ ions with g slightly greater than 2, and a Weiss constant, θ, = -8.2(4) K, in agreement with dominant antiferromagnetic interactions in the sample. The χT(T) data are in good agreement with the χT value plateauing just below 2.0 at high temperature.

Initial attempts to model the magnetic properties for this system were made using an ideal tetrahedral geometry with a single isotropic superexchange, with coupling constant J [22], between each pair of Cu(II) ions bridged by the O^{2-} ion. These attempts proved unsuccessful and failed to capture the χT values observed below 80 K. In addition, this model overestimated the magnetization values at higher fields, but was satisfactory for low field values. Instead, a similar approach that was presented in [18] was employed for our system. This more complicated model considers anisotropy in the superexchange coupling, as is suggested in the presented magnetic measurements. The construction of this model assumes an ideal tetrahedral geometry, where Cu(II) ions are placed at each vertex of a tetrahedron and the oxygen ion is located at the center. We define a local coordinate frame $(\alpha_i, \beta_i, \gamma_i)$ with $i = 1, 2, 3, 4, 5,$ and 6 for each of the coupled Cu(II) ions as illustrated in Figure 6. As part of this coordinate frame we will define the unit vectors; $\hat{e}_{\alpha_i}$ which points in a direction linking the Cu(II) ions, $\hat{e}_{\beta_i}$ in the Cu-O-Cu plane pointing toward the oxygen, and $\hat{e}_{\gamma_i}$ as $\hat{e}_{\alpha_i} \times \hat{e}_{\beta_i}$. These directions have been previously described as apical for the direction given by $\hat{e}_{\gamma_i}$ and equatorial for the directions given by $\hat{e}_{\alpha_i}$ and $\hat{e}_{\beta_i}$ [18]. We will use the same labeling scheme for this work, so that $J_1 = J_{ap}$ and $J_2 = J_{eq}$.

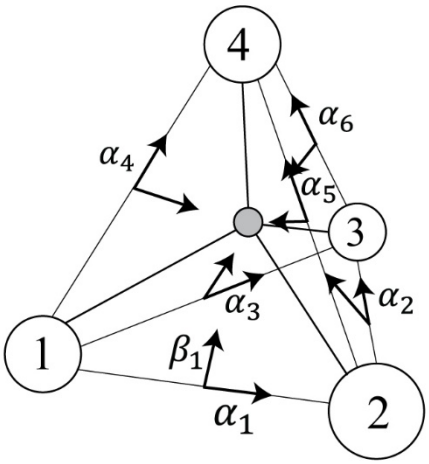

Figure 6. Graphical illustration of idealized geometry for the Cu(II) cluster. The sets of arrows represent the local coordinate frame $(\alpha_i, \beta_i, \gamma_i)$. For clarity only α_i and β_i are drawn, γ_i can be determined by $\alpha_i \times \beta_i$.

As a result, we can now write our Hamiltonian as,

$$\widehat{H} = J_{ap} \sum_{i=1}^{6} \hat{S}_{\gamma_i(1)} \cdot \hat{S}_{\gamma_2(2)} + J_{eq} \sum_{i=1}^{6} \left(\hat{S}_{\alpha_i(1)} \cdot \hat{S}_{\alpha_i(2)} + \hat{S}_{\beta_i(1)} + \hat{S}_{\beta_i(2)} \right) + g\mu_B \vec{H} \cdot \sum_{j=1}^{4} \hat{S}_j \qquad (1)$$

where the first two terms refer to the anisotropic superexchange interactions between the Cu(II) ions in the local apical and equatorial directions respectively where $J_{ap} \neq J_{eq}$ and last term is the Zeeman coupling of the Cu(II) ions with the external magnetic field. A 16×16 symbolic Hamiltonian matrix was constructed from Eq. (1) and diagonalized to produce the energy eigenvalues of the system. These were used to construct the Partition function equation. A MATLAB script was created to simultaneously numerically differentiate the Partition function with respect to magnetic field to obtain magnetic susceptibility multiplied by temperature and fit the resulting equation to the experimental χT data varying parameters J_{ap}, J_{eq}, and g using a least-squares curve fitting technique. This fit yielded the convergent results of $J_{ap}/k_B = -61.1(7)$K, $J_{eq}/k_B = 41.2(3)$K, and $g = 2.27(9)$ with the susceptibility and magnetization best fits plotted against the experimental data presented in Figure 7.

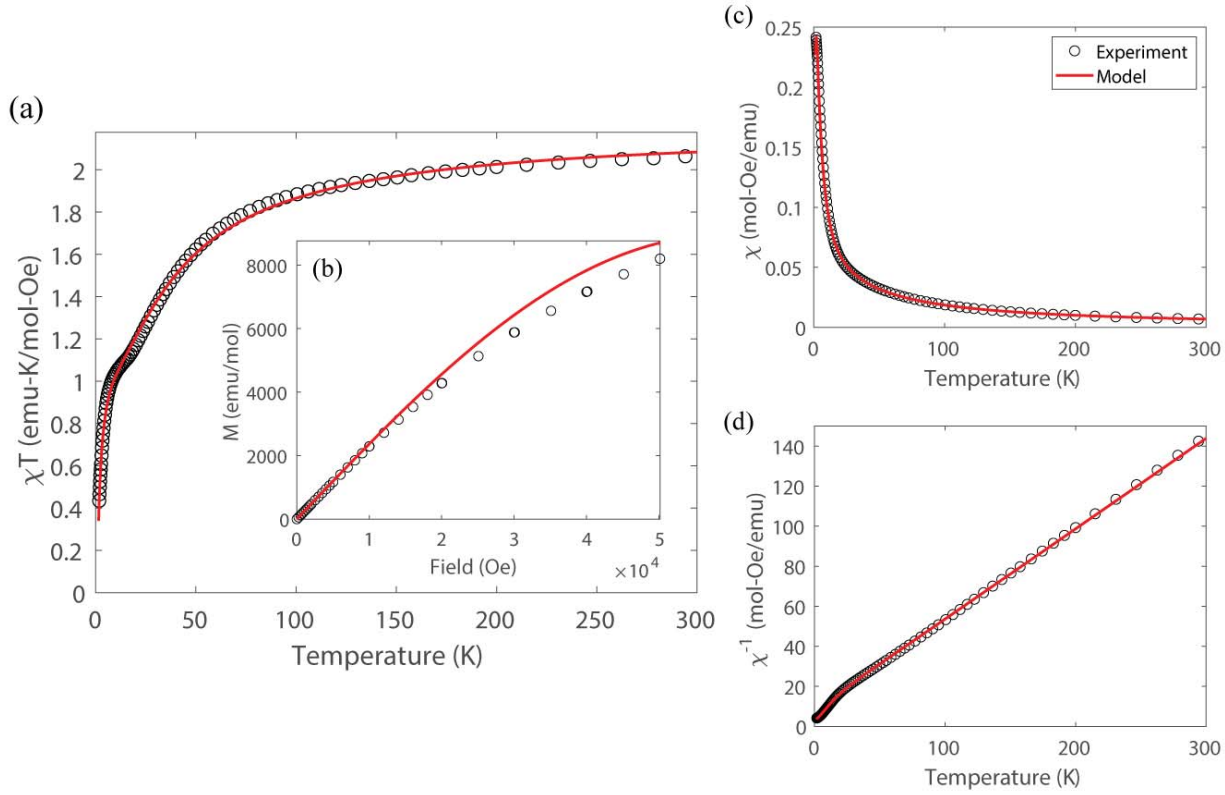

Figure 7. Susceptibility and magnetization best fit (solid lines) compared with experimental data (symbols) for (a) $\chi T(T)$, (b) $M(H)$, (c) $\chi(T)$, and (d) $\chi^{-1}(T)$.

The resulting fits reveal that the superexchange couplings between the Cu(II) ions are highly anisotropic and differ in sign. The apical coupling was found to be ferromagnetic and the

equatorial coupling is antiferromagnetic which agrees previously reported results for similar tetrahedral Cu(II) systems [23, 24, 25, 26]. The fitted value for the spectroscopic factor g is also reasonable for Cu(II) ions. Despite the simplification of this model and it being reported as a first order approximation, the fitted results were acceptable for this particular case due to the nearly tetrahedral geometry of our system and the cluster isolation.

Discussion

Antiferromagnetically ordered lattices all have unique, singlet ground states. If structural constraints prevent the formation of such a ground state, no matter how strong the interactions, the system is said to be geometrically frustrated. Consider, for example, a simple equilateral triangle of magnetic moments confined to one axis (Figure 8). If one moment (A) is arbitrarily assigned to 'up', the adjacent moment (B) will adopt a 'down' orientation to satisfy the preferred singlet state of the antiferromagnetic exchange. The problem lies with the third moment (C), which by symmetry must be antiparallel to both of the prior two moments which are themselves are mutually antiparallel – an impossible conundrum which gives rise to two degenerate ground states, i.e. frustration.

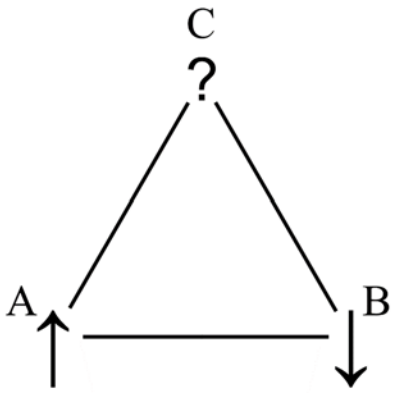

Figure 8 – A simplified model of three magnetic moments arranged as an equilateral triangle.

A somewhat different problem arises in the tetrahedral cluster of copper ions in the adamantoid structure, in which the four moments share identical interactions (consider a fourth moment D in the center of Figure 8, raised above the plane). Pair A and C may align antiferromagnetically, as may pair B and D, but each pair is independent of the other. Consequently, there are multiple sets of possible S = 0 ground states (for example AB/CD, AD/BC) and no long-range order is possible.

Frustration can be eliminated if the symmetry of the lattice is lowered. This can occur by the application of an external magnetic field or uniaxial pressure applied to the crystal. Grain boundaries, or impurities in the magnetic sites have also been shown to induce order [27]. It is possible for frustration to strain the lattice sufficiently to induce a structural phase change, (as occurs during a spin-Peierls transition [28].

Although the symmetry of **1** is high (space group *P4/n*) with a single oxide ion and all Cu ions equivalent by symmetry, there are two crystallographically unique chloride ions, one of which is two-site disordered. This leads to several slightly different potential superexchange pathways. The Cu-O bond length is constant and the Cu-O-Cu angles are the same within experimental error. However, the Cl-Cu-Cl angles vary by up to 2.7° which, while a small variation, would be expected to cause slight changes in the magnetic exchange. Whether that difference is sufficient to be observed experimentally depends upon the difference in the magnitude of the exchange via the chloride ions and the central oxide ion. The agreement between the calculations and experimental data is quite strong, but some differences are observed which may arise due to the slight reduction in symmetry or possible exchange between molecules through the short Cl···Cl contacts. The possibility of a low temperature phase transition (similar to the Spin-Peierls transition) cannot be discounted, but given the absence of any discontinuities in the data, such a transition must be second order in nature.

Summary

The synthesis and structural characterization of a new copper chloride adamantoid structure is reported. The compound crystallizes in the tetragonal space group *P4/n* which provides for a limited number of potential magnetic superexchange pathways. Variable temperature magnetization measurements were modeled using a two exchange parameter approach with an additional term to account for the Zeeman interaction of the Cu(II) ions with the applied field. This resulted in both antiferromagnetic (dominant) and ferromagnetic contributions to the exchange of $J_{ap}/k_B = -61.1(7)\text{K}$ and $J_{eq}/k_B = 41.2(3)\text{K}$ in good agreement with previously reported compounds. More detailed analyses of additional members of this family are in progress.

Supplementary Information:

CCDC 2249833 contains the supplementary crystallographic data (CIF). These data can be obtained free of charge via https://www.ccdc.cam.ac.uk/structures/, or from the Cambridge Crystallographic Data Centre, 12 Union Road, Cambridge CB2 1EZ, UK; fax: (+44) 1223-336-033; or e-mail: deposit@ccdc.cam.ac.uk.

Acknowledgments

Financial support from the NSF (IMR-0314773) toward the purchase of the SQUID magnetometer, SEQENS toward the purchase of the powder X-ray diffractometer and The Kresge Foundation toward the purchase of both, is gratefully acknowledged. BAM is grateful for a SEQENS Summer Undergraduate Research Fellowship. In addition, the authors are grateful to the NSF for support of the purchase and construction of a helium recycling system (DMR-1905950). Dr. Alistair D. Richardson is acknowledged for work in the initial preparation of compound **1**.

References

1. J.A. Bertrand and J. Kelley, *J. Am. Chem. Soc.* **88**, 4746 (1966).

2. a) R. Vafazadeh, N. Hasanzade, M. M. Heidari, and A.C. Willis, *Acta Chim. Slov,* **62**, 2015, 122 (2015). b) M.A. El-Sayed, A. Ali, G. Davies, S. Larsen, J. Zubieta, *Inorg, Chim, Acta* **194**, 139 (1992). c) R.C. Dickinson, F.T. Helm, W.A. Baker, Jr., T.D. Black, and W.H. Watson, Jr., *Inorg, Chem,* **16**, 1530 (1977).

3. a) F. Bottomley, P.D. Boyle, S. Karslioglu, R.C. Thompson *Organometallics* **12**, 4090 (1993). b) T.S. Lobana, P. Kaur, T. Nishioka *Inorg. Chem*. **43**, 3766 (2004). c) X.-M. Zhang, J.-J. Hou, C.-H. Guo, C.-F. Li *Inorg. Chem*. **54**, 554 (2015). d) L.-X. Hu, F. Wang, Y. Kang, J. Zhang *Cryst. Growth Des*. **16**, 7139 (2016).

4. a) S. Becker, M. Durr, A. Miska, J. Becker, C. Gawlig, U. Behrens, I. Ivanovic-Burmazovic, and S. Schinder, *Inorg. Chem.* **55**, 3659 (2016). b) K. Skorda, T.C. Stamatatos, A.P Vafiadia, A.T. Lithoxoidou, A. Terzis, S.P. Perlepes, J. Mrozinski, C.P. Raptopoulou, J.C. Plakatouras, E.G. Balkalbassis, *Inorg. Chim. Acta* **358**, 565 (2005).

5. Z. Cui, Y. Ma, Y. Ling, X. Yang, *X-ray Struct. Anal. Online* **25**, 79 (2009).

6. P. De Vreese, N. R. Brooks, K. Van Hecke, L. Van Meervelt, E. Matthijs, K. Binnemans, R. Van Deun, *Inorg. Chem.* **51**, 4972 (2012).

7. M. Jansen, B. Luer, *Z. Kristallographie*, **177**, 149 (1986).

8. a) E. Śliwa, D. Nesterov, M. Kirillova, J. Kłak, A. Kirillov, and P. Smoleński, *Inorg. Chem*. **60**, 9631 (2021). b) O. Zaharko, P.J. Brown, M. Mys'kiv, *Phys. Rev. B* **81**, 172405 (2010). c) A. Mishra, S. Verma, *Inorg. Chem. Commun.* **49**, 3691 (2010).

9. I.P.Kondratyuk, M.A.Yampol'skaya, Yu.A.Simonov, L.A.Muradyan, V.I.Simonov, *Kristallogr.* **31**, 682 (1986).

10. G. A. Bowmaker, C. D. Nicola, C. Pettinari, B.W. Skelton, N. Somers, A.H. White, *Inorg. Chim. Acta* **375**, 31 (2011).

11. a) A.D. Richardson, T.J. Zirkman, M.T. Kebede, C.P. Landee, R. Rademeyer, M.M. Turnbull, *Polyhedron*, **147**, 106-19 (2018). b) L. Macek, J.C. Bellamy, K. Faber, C.R. Milson, C.P. Landee, D.A. Dickie, M.M. Turnbull. *Polyhedron* **229**, 116214 (2023). c) C.P. Landee, F.F. Awwadi, B. Twamley, M.M. Turnbull *J. Coord. Chem*. **75**, 2616 (2022). d) A. Araujo-Martinez, C.P. Landee, D.A. Dickie, J.L. Wikaira, F. Xiao, M.M. Turnbull, *J. Coord. Chem*. **76**, in press (2023).

12. Carlin, R. L., *Magnetochemistry,* Springer-Verlag, Berlin, **1986**.

13. SAINT. Ver. 8.34A. (Bruker-AXS, 2014).

14. G. Sheldrick, SADABS, University of Göttingen, Germany, 1996.

15. G.M. Sheldrick *Acta Cryst. A,* **64**, 112 (2008).

16. G.M. Sheldrick *Acta Cryst. C*, **C71**, 3 (2015).

17. MATLAB. 9.7.0.1190202 (R2019b). Natick, Massachusetts: The MathWorks Inc.; 2018.

18. N. Hfidhi, O. Kammoun, R. Pelka, M. Fitta, H. Naïli, *Inorg. Chim. Acta* **469**, 431 (2018).

19. S. Wang, E.E. Morgan, S. Panuganti, L Mao, P. Vishnoi, G. Wu, Q. Liu, M.G. Kanatzidis, R.D. Schaller, R. Seshadri *Chem. Mater*. **34**, 3206 (2022).

20. A.W. Addison, N.T. Rao, J. Reedijk, J. van Rijn, G.C. Verschoor, *J. Chem. Soc., Dalton Trans.* 1349 (1984).

21. a) R. Dickinson, F. Helm, W. Baker, Jr., T. Black, and W. Watson, Jr., *Inorg. Chem.* **16**, 1530 (1977). b) C. Richardson and P.J. Steel, *Dalton Trans.* 992 (2003).

22. J.T. Haraldsen, T. Barnes, J. L. Musfeldt *Phys. Rev. B* **71**. 064403 (2005).

23. T. Moriya, *Phys. Rev.* **120**, 91 (1960).

24. M.E. Lines, A.P. Ginsberg, R.L. Martin, R.C. Sherwood *J. Chem. Phys.* **57**, 1 (1972).

25. R.C. Dickinson, F.T. Helm, W.A. Baker, T.D. Black, W.H. Watson *Inorg. Chem.* **16**, 1530 (1977).

26. E.I. Śliwa, D.S. Nesterov, M.V. Kirillova, J. Kłak, A.M. Kirillov, P. Smoleński *Inorg. Chem.* **60**, 9631 (2021).

27. D.P. Kozlenko, A.F. Kusmartseva, E.V. Lukin, D.A. Keen, W.G. Marshall, M.A. de Vries, K. V. Kamenev Phys. Rev. Lett., **108**, 187207 (2012).

28. J.W. Bray, L.V. Interrante, I.S. Jacobs, J.C. Bonner, "The Spin-Peierls Transition" In: J.S. Miller (ed) *Extended Linear Chain Compounds.* (1983) Springer, Boston, MA.